Mineralogical Magazine, August 2003, Vol. 67(4), pp. 799–806

Textural and spectroscopic studies on hydrothermal dumortierite from an Al-rich clay deposit, southeastern Korea

C. O. CHOO* AND Y. KIM

Department of Geology, Kyungpook National University, Daegu, 702-701, Korea

ABSTRACT

Dumortierite occurs as small nodules or thin layers along horizontal fractures in the altered volcanic rocks of the Milyang clay deposit, southeastern Korea. Textural evidence shows that dumortierite is associated with pyrophyllite, suggesting that the silica activity increased with decreasing B and Al activities during the hydrothermal alteration. Dumortierite chemistry shows a slight excess of Al, possibly due to common occurrence of Al-rich minerals in the clay deposit. The structural formula of dumortierite is recalculated as $Al_{6.93}(Fe_{0.03}Mg_{0.07})B(Si_{2.99}Al_{0.01})O_{18}$. An absorption peak at 1387 cm^{-1} in the IR spectrum indicates that B is present in three-fold coordinated sites. The ^{29}Si MAS NMR spectrum has two peaks at −90.9 and −95.5 ppm, showing that Si in dumortierite is located in two different crystallographic sites and is linked to four octahedral Al atoms. The ^{27}Al MAS NMR spectrum shows only one asymmetrical peak near 0 ppm, suggesting that there is no substitution of Al for Si. The ^{11}B MAS NMR spectrum at 17.5 ppm shows a typical second order quadrupole pattern represented by the three-fold coordinated B. The ^{11}B chemical shifts indicate that all of the B occupies such sites, indicating that the B sites are axially symmetric or nearly so in a very well defined site.

KEYWORDS: dumortierite, clay deposit, boron, trigonal group, MAS NMR, Korea.

Introduction

DUMORTIERITE is the most abundant mineralogical sink for B after tourmaline. Boron is noted for being a mobile element in many geochemical environments and any introduction of B into a system will potentially produce dumortierite as well as tourmaline (e.g. Henry and Dutrow, 1996). Dumortierite commonly occurs in rocks such as pegmatite and aplite, in acidic dykes and in granitic rocks (Huijsmans *et al.*, 1982), late-stage pneumatolytic deposits or hydrothermal deposits (Kerr and Jenney, 1935; Sabzehei, 1971; Foit *et al.*, 1989), and regional metamorphic rocks up to very high grades (Schreyer *et al.*, 1975; Takahata and Uchiyama, 1985; Beukes *et al.*, 1987; Chopin *et al.*, 1995). The dumortierite group consists of two types of minerals, namely, dumortierite and magnesiodumortierite. The transition from dumortierite to Ti-free magnesiodumortierite is favoured by increasing pressure (Chopin *et al.*, 1995).

Spectroscopic methods such as magic angle spinning nuclear magnetic resonance (MAS NMR) and infrared (IR) spectroscopy may be more accurate than conventional X-ray diffraction (XRD) in structural interpretations of dumortierite. The NMR, in particular, has proven to be a useful tool in investigating the local structure of silicate minerals. ^{29}Si and ^{27}Al are the two main isotopes which are successfully applied and mostly used in mineralogy and geochemistry (Kirkpatrick, 1988). Other isotopes including alkali cations and ^{11}B have been also studied (Turner *et al.*, 1986; Kim and Kirkpatrick, 1998). ^{11}B is a good candidate for NMR study because it has 100% natural abundance (spin number I = ⅔) and easily differentiates three- and four-fold coordinated B in minerals (Turner *et al.*, 1986). It also provides information on the B symmetry. Recently, ^{11}B MAS NMR was used to verify the existence of B in four-fold coordination in

* E-mail: chooco@hanmir.com
DOI: 10.1180/0026461036740136

tourmaline (Tagg *et al*., 1999). Dumortierite has not previously been studied by NMR. Boron in dumortierite has been assumed to be present in three-fold coordination (Tagg *et al*., 1999), but no spectroscopic study has been carried out to support that assumption.

Dumortierite occurs in the Milyang clay deposit, southeastern Korea (Lat. 35°30′N–35°32′N and Long. 128°41′E–128°47′E). This clay deposit is characterized by the common occurrence of Al-rich minerals composed predominantly of pyrophyllite, dickite and diaspore with accessory minerals such as quartz, tosudite, illite, tourmaline, dumortierite, andalusite, wavellite, baryte and pyrite (Kim *et al*., 1992; Lee *et al*., 1993; Koh *et al*., 2000). The aim of the present study is the investigation of textural and spectroscopic features of dumortierite formed at an Al-rich clay deposit developed in volcanic rocks.

Occurrence of dumortierite

In southeastern Korea, several clay deposits were formed by hydrothermal alteration of the Yucheon volcanic rocks affected by intrusion of the Bulguksa Granite of late Cretaceous to early Tertiary. The Yucheon volcanic rocks are 75–64 Ma old (Min *et al.*, 1982) and the Bulguksa Granite, derived from I-type magma, with calc-alkaline series are 66.5–62 Ma (Hong and Choi, 1988; Jin *et al*., 1991), respectively. There have been many geochemical and mineralogical studies on the Milyang clay deposit (Kim *et al*., 1992; Lee *et al*., 1993; Oh and Chon, 1993; Koh and Chang, 1997, Koh *et al*., 2000, Choo *et al*., 2001). Using K-Ar age dating, the hydrothermal alteration age of this clay deposit has been measured as 69.7±2.1 Ma (Koh *et al*., 2000). The deposit is known to have formed in late-Cretaceous andesitic tuff by hydrothermal alteration, possibly associated with subsequent intrusion of adjacent granite.

Dumortierite occurs as small nodules or thin layers along horizontal fractures in the altered volcanic rocks. Dumortierite nodules are a few mm in diameter and dumortierite layers are <2 cm thick. Dumortierite nodules contain a concentric growth texture with a cobalt blue hue, especially in the outermost and innermost growth layers. Under stereomicroscopic observation, dumortierite commonly forms bundles, needles or fibrous aggregates with a radial texture. Radiating dumortierites are closely associated with pyrophyllite. Distinctive optical properties are strong pleochroism and negative elongation under the polarizing microscope.

Analytical methods

X-ray diffraction analysis in the identification of and in the calculation of cell dimensions for dumortierite was performed using a Rigaku Geigerflex RAD3-C with Ni-filtered Cu-$K\alpha$ radiation. The XRD data were recorded at 40 kV and 30 mA by counting at 3 s intervals steps of 0.02°2θ, from 5 to 65°2θ. Field emission scanning electron microscopy (FESEM) observations were performed on the fresh surfaces of materials using Hitachi model S-4200 equipped with an energy-dispersive spectrometer (EDS). Electron microprobe analysis (EMPA) was performed on polished petrographic thin-sections using a Shimazu 1600 Electron Microprobe equipped with four channels wavelength-dispersive spectrometers (WDS). Backscattered electron (BSE) images were obtained from the polished thin sections after carbon coating using the same microprobe. Quantitative chemical analysis was performed by EMPA fitted with automated WDS operated at 1 μm beam diameter, 15 kV accelerating voltage and 10 nA beam current. The chemical results were calculated using a ZAF correction and Fe was assumed as ferrous, and cation numbers were normalized on the basis of 18 oxygens. Due to analytical limitations for B by EMPA, the B_2O_3 contents were fixed as a unit by assuming full occupancy of the B site per formula unit and thus the weight percent of B_2O_3 was correspondingly recalculated. Such assumptions could yield satisfactory data when analysing borosilicates (Alexander *et al*., 1986; Werding and Schreyer, 1990; Visser and Senior, 1991; Henry and Dutrow, 1996; Aurisicchio *et al*., 1999; Platonov *et al*., 2000).

Magic angle spinning nuclear magnetic resonance was applied to the interpretation for important cation sites in the dumortierite structure. ^{29}Si, ^{27}Al and ^{11}B MAS NMR spectra were collected at 59.6, 78.2 and 96.3 MHz using a 300 MHz Varian FT NMR. The samples were spun at 6 kHz. Single pulse excitation with pulse width of 1 μs was used with a 5 s delay for ^{29}Si, 3 μs with 5 s delay for ^{11}B and 4 μs with a 1 s delay for ^{27}Al. The chemical shifts are reported in parts per million (ppm) relative to external tetramethylsilane (TMS) for ^{29}Si, 1 M $AlCl_3$ solution for ^{27}Al, and B trifluoride diethyl etherate (BF_3Oet_2) for ^{11}B. The experimental line shapes

of ^{11}B MAS NMR were simulated by the method of Lippmaa *et al.* (1986). A Bruker IFS120 HR Fourier Transform Infrared (FTIR) spectrometer was used in order to characterize B and OH groups in dumortierite using pellets of a mixture of KBr plus the mineral powder in the range 4000–400 cm^{-1} with a resolution of 0.5 cm^{-1}.

Results and discussion

Crystal chemistry of dumortierite

Dumortierite was once considered to be anhydrous $Al_7BSi_3O_{18}$, but spectroscopic analysis has revealed the presence of hydroxyl groups (Moore and Araki, 1978; Alexander *et al.*, 1986; Werding and Schreyer, 1990). Moore and Araki (1978) proposed 0.75 OH per formula unit, though Alexander *et al.* (1986) and Platonov *et al.* (2000) suggested different hydroxyl contents, e.g. 0.6 OH. The total amount of OH varies not only with the number of octahedral vacancies but also with the divalent ions such as Mg, Ca, Fe^{2+} and tetravalent substituent for octahedral Al and trivalent substituent for tetrahedral Si (Alexander *et al.*, 1986; Werding and Schreyer, 1990). The Milyang dumortierite contains negligible Fe, Mg and Ti. For comparison, magnesiodumortierite commonly has these elements up to a few percent (Visser and Senior, 1991). Our sample may contain some hydroxyl, as shown by IR spectroscopy. The structural formula of dumortierite is recalculated as $Al_{6.93}(Fe_{0.03}Mg_{0.07})B(Si_{2.99}Al_{0.01})O_{18}$. The fact that Al is slightly excessive per formula unit can be explained by the common association with other Al-rich minerals such as diaspore, dickite, pyrophyllite, tourmaline and andalusite in the Milyang clay deposit. Likewise, dumortierite is frequently associated with Al-rich minerals such as andalusite (Taner and Martin, 1993), or cordierite (Kerr and Jenney, 1935; Visser and Senior, 1991). Based on the classification of colours by the ratio Fe/(Fe+Ti) in dumortierite (Alexander *et al.*, 1986), the chemistry of the Milyang dumortierite lies in the blue colour region, consistent with colour description in the field. The Fe and Ti are responsible for the blue or pink colour of dumortierite, depending on the relative importance of Fe^{2+}-Fe^{3+} and Fe^{2+}-Ti^{4+} charge transfers, respectively (Alexander *et al.*, 1986).

The strongest dumortierite XRD reflection is at 5.91 Å with moderately strong reflections at 5.11 Å, 3.45 Å, 2.98 Å, 2.55 Å and 2.11 Å. By use of least-squares refinement, the calculated cell dimensions of dumortierite are a = 11.71 Å, b = 20.39 Å, c = 4.70 Å and V = 1129.48 $Å^3$, respectively. Alexander *et al.* (1986) calculated a range of dimensions with values varying as follows: a = 0.021 Å, b = 0.055 Å, c = 0.018 Å and V = 7.7 $Å^3$ from twelve dumortierites collected because cell dimensions vary with crystal chemistry. Chopin *et al.* (1995) measured unit-cell dimensions of magnesiodumortierites: a = 11.91 Å, b = 20.40 Å, c = 4.730 Å and V = 1149 $Å^3$ for single crystal, and a = 11.91 Å, b = 20.42 Å, c = 4.714 Å and V = 1146 $Å^3$ for powder data, respectively. The a axis and cell volume of magnesiodumortierites are slightly larger than those of common dumortierites possibly due to substitution of Fe, Mg and Ti for Al. The fact that cell parameters of the Milyang dumortierite are relatively small is possibly due to the influence of excess Al in octahedral sites.

Textural features by SEM and BSE images

Dumortierites consist of radiating fibres or acicular aggregates (Fig. 1*a*). Some are a few μm wide, but, in rare cases, others are up to tens of μm wide. They show different orientation depending on each packet, suggesting competition during the crystal growth (Fig. 1*b*). Backscattered electron (BSE) images reveal that dumortierite composed of radiating fibres was altered to pyrophyllite (Fig. 2*a*), indicating that dumortierite was unstable with respect to pyrophyllite. Note that radiating dumortierite and decomposed tourmaline are together found in the pyrophyllite matrix (Fig. 2*b*). Tourmaline relics are easily found in the pyrophyllite matrix and around the marginal parts of dumortierite. There is no compositional zoning in dumortierite, but weak zoning in tourmaline. Therefore it is evident that the stages at which borosilicate minerals dumortierite and tourmaline grew were considerably different from each other. A mixed phase where dumortierite significantly altered to pyrophyllite is shown in Fig. 3. Very small crystals of pyrophyllite grew on the steps or edges of dumortierite. The grain boundaries between the two minerals are relatively obscure and they are densely compacted.

Because textural evidence shows that tourmaline was predated by dumortierite, the breakdown of tourmaline as a precursor might have supplied the B for the dumortierite formation. Otherwise, it is possible that dumortierite formed at the expense

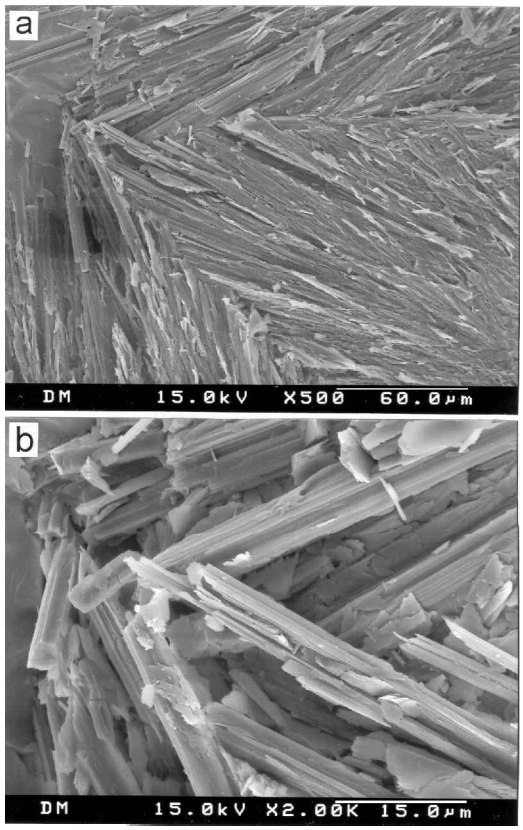

FIG. 1. SEM images of dumortierite. (*a*) Radiating dumortierite. (*b*) Enlarged portion of part *a*.

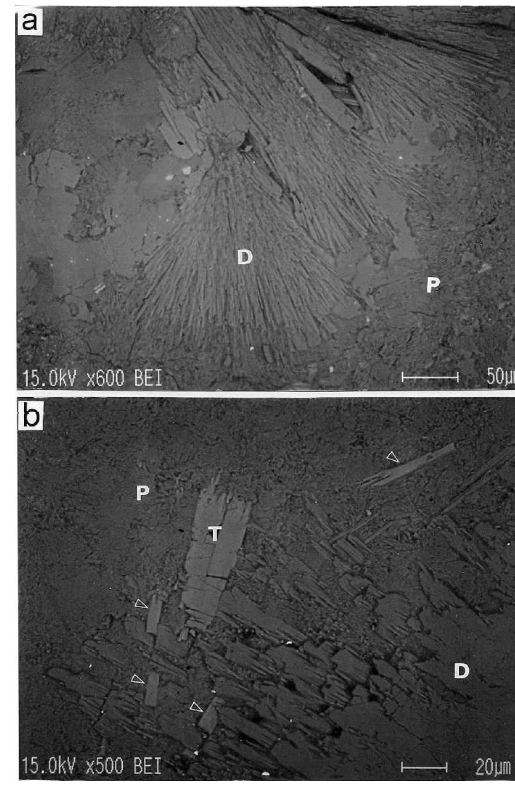

FIG. 2. BSE images showing dumortierite (D) and associated minerals. (*a*) Radiating dumortierite in the pyrophyllite (P) matrix. (*b*) Dumortierite and tourmaline (T) decomposed. The arrows indicate relics of tourmalines.

of tourmaline owing to the marked depletion of Fe and Mg prior to the addition of B. The fact that dumortierite is closely associated with pyrophyllite suggests that the silica activity increased with decreasing B and Al activities during the hydrothermal alteration. Boron was probably introduced early in the episode of hydrothermal alteration. Formation of dumortierite, together with tourmaline, may have involved leaching of Al from silicate wallrocks under high water/rock conditions in order to precipitate these aluminous minerals (Slack, 1996). The Al activity in melt appears to be among the important parameters for dumortierite stability and requires a higher total concentration of Al to promote dumortierite growth and the presence of Al favours the fractionation of B into the minerals (Werding and Schreyer, 1996). Such an implication is supported by the common occurrence of diaspore, dickite and pyrophyllite as major minerals in this clay deposit. The presence of dumortierite in a hydrothermal clay deposit suggests an important role for B in acidic volcanic rocks that show evidence of Al-rich mineralization.

Spectroscopic data

According to the FTIR spectrum (Fig. 4), the hydroxyl-stretching vibration with a large broad peak occurs at 3492.5 cm^{-1}, which indicates that the hydroxyl group is incorporated loosely in the structure. A strong absorption peak at 1386.6 cm^{-1} indicates that B is present in threefold coordination as part of a planar BO_3 group, namely BO_3. Since the spectrum related to the threefold coordinated B is nearly symmetrical, it is suggested that all B in dumortierite is in threefold coordination.

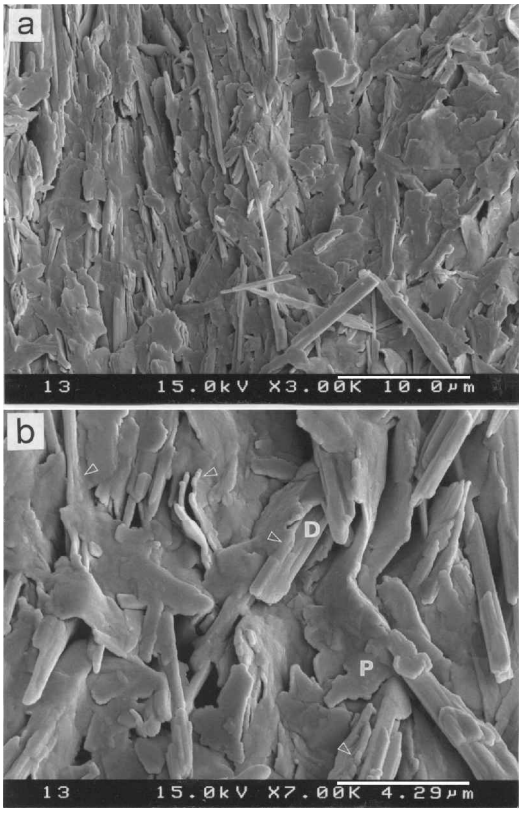

FIG. 3. SEM images. (*a*) Dumortierite intensely altered to pyrophyllite. (*b*) Small crystals of pyrophyllite (P) grew on the steps or edges of dumortierite (D). Note the arrows showing that grain boundaries between the two minerals are relatively obscure.

The MAS NMR may be more accurate than IR in interpreting important cation sites in the dumortierite structure. For silicate minerals, the empirical relationships between ^{29}Si chemical shifts and structural and chemical parameters are well known (Kirkpatrick, 1998). Recently, *ab initio* calculations have been used successfully to gain an insight into these correlations (Xue and Kanzaki, 1998). The most important correlations for ^{29}Si are the Si–O–Si angle and the mean Si–Si distance per tetrahedron for SiO_2 phases, polymerization of Si (next neighbour, NN) for silicates, the number of tetrahedral Al next-nearest neighbours (NNN) for aluminosilicates, and other structural effects. The ^{29}Si MAS NMR spectra of most framework aluminosilicates with more than one crystallographic tetrahedral site are not well resolved because of peaks from Si on different sites with different numbers of Al next-nearest neighbours (NNN) and only a few have been reported to have resolved peaks (Putnis *et al.*, 1985).

Figure 5 shows the MAS NMR spectra for dumortierite. The ^{29}Si MAS NMR spectrum shows two peaks from dumortierite at −90.9 and −95.5 ppm. It also contains one sharp peak from quartz as an impurity in our sample and some low-intensity peak which cannot be identified. The Si in dumortierite is located in two different crystallographic sites and is linked to four octahedral Al atoms. Therefore, ^{29}Si MAS NMR peaks in dumortierite do not have disordered Al around Si, showing two separate peaks for two different Si sites at −90.0 and −95.5 ppm. Our dumortierite is not pure and most

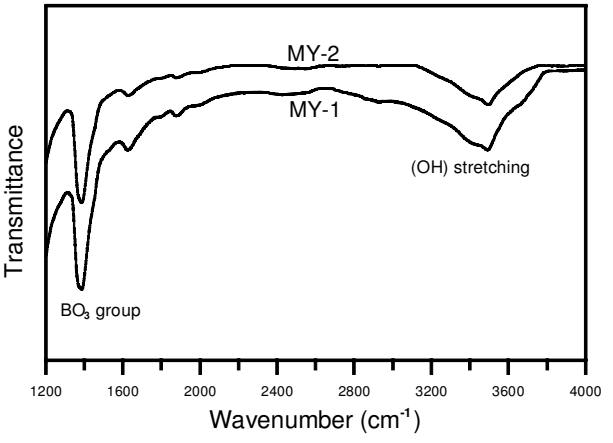

FIG. 4. FTIR spectrum showing a hydroxyl group and a BO_3 group in two dumortierite samples.

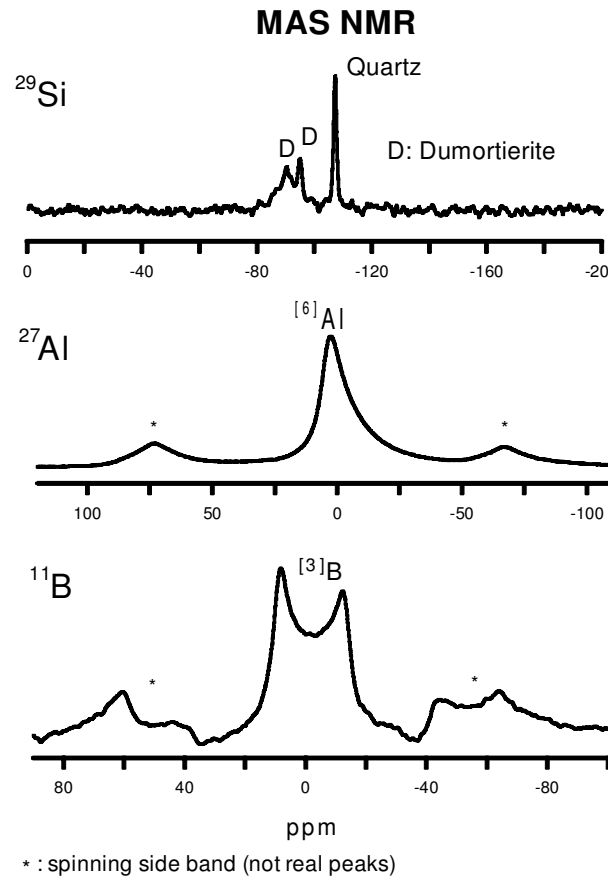

FIG. 5. MAS NMR spectra of dumortierite showing ^{29}Si, ^{27}Al and ^{11}B peaks, respectively.

of the impurities are of quartz and clay minerals, represented by the peak at −107.8 ppm and some other low-intensity peaks. The width of the −90.0 ppm peak is broader than that at −95.5 ppm, probably due to the overlap with peaks related to impurities.

The ^{27}Al MAS NMR spectrum has only one asymmetrical peak near 0 ppm without second-order quadrupolar line shape, suggesting that there is only octahedral Al without substitution of Al for Si and also indicating that there is a distribution in the isotropic chemical shift and the quadrupole interaction (Kentgens, 1997). Dumortierite has four crystallographically different Al atoms with different bond lengths, leading to this kind of pattern.

The ^{11}B MAS NMR spectrum shows a typical second-order quadrupole pattern represented by the threefold coordinated B. Simulation results show that the threefold coordinated B has its isotropic chemical shift at 17.5 ppm, quadrupole coupling constant (e^2Qq/h) 2.75 MHz, and asymmetry parameter (η) 0.1. The one ^{27}Al MAS NMR peak near 0 ppm (octahedral Al) suggests that there is no substitution of Al for Si.

In natural minerals, B can exist in both three- and four-fold coordination and it can be verified easily by NMR (Turner *et al.*, 1985). Boron in dumortierite has been assumed to be in a trigonal form, but no direct spectroscopic study has been performed to support that idea. By comparison, tourmaline is assumed to contain B in thre-fold coordination, but a recent study by Tagg *et al.* (1999) showed that some of the excess B in tourmaline exists in tetrahedral form. Spectroscopic investigations by Schreyer *et al.* (2000) proved that B occurs not only in three-fold coordination but is also located in the tetrahedral

ring site of the synthetic tourmaline (olenite). The ^{11}B chemical shifts at 17.5 ppm for our dumortierite sample, however, indicate that B is entirely in three-fold coordination, unlike some tourmalines. The ^{11}B NMR peak is broad and has a typical second order quadrupole pattern with very small asymmetry parameter (η, 0.1), showing that trigonal B in dumortierite is axially symmetric or nearly so in a very well defined site. Our spectroscopic results obtained from FTIR and MAS NMR indicate that only three-fold coordinated B is present in dumortierite.

Conclusions

From the textural evidence, we conclude that dumortierite formed during the early stages of hydrothermal alteration, and later, pyrophyllite formed with the addition of silica. Dumortierite was unstable with respect to pyrophyllite as hydrothermal alteration proceeded. The silica activity increased with decreasing B and Al activities during the hydrothermal alteration. Because textural evidence shows that tourmaline was predated by dumortierite, the breakdown of tourmaline as a precursor might have supplied the B for the formation of dumortierite. The presence of dumortierite suggests an important role for B in hydrothermal alteration and clay mineralization. Spectroscopic results obtained from FTIR and MAS NMR indicate that B in dumortierite is present only in three-fold coordination, as part of a planar BO_3 group. However, spectroscopic and chemical data for more samples further need to be investigated in order to better understand the crystal chemistry of dumortierite in association with Al-rich minerals.

Acknowledgements

This research was partially supported by the Brain Korea 21 project donated to KNU. Instrumental analyses were carried out at the Daegu Branch of Korea Basic Sciences Institute (KBSI). Helpful comments by reviewers led to substantial improvements in the manuscript.

References

Alexander, V.D., Griffen, D.T. and Martin, T.J. (1986) Crystal chemistry of some Fe- and Ti-poor dumortierites. *American Mineralogist*, **71**, 786–794.

Aurisicchio, C., Ottolini, L. and Pezzotta, F. (1999) Electron- and ion-microprobe analyses, and genetic inferences of tourmalines of the foite-schorl solid solition, Elba Island (Italy). *European Journal of Mineralogy*, **11**, 217–225.

Beukes, G.J., Slabbert, M.J., de Bruiyn, H., Botha, B.J.V., Schoch, A.E. and van der Westhuizen, W.A. (1987) Ti-dumortierite from the Keimoes area, Namaqua mobile belt, South Africa. *Neues Jahrbuch für Mineralogie Abhandlungen*, **157**, 303–318.

Choo, C.O., Kim, J.J. and Kim, Y. (2001) Complex zoned tourmaline in the diaspore nodule from a hydrotherrmal kaolin deposit, Miryang deposit, south Korea. *11th Annual Goldschmidt Conference, May 2001, Virginia, USA.* Abstract supplement, 147.

Chopin, C., Ferraris, G., Ivaldi, G., Schertl, H.-P., Schreyer, W., Compagnoni, R., Davidson, C. and Davis, A.M. (1995) Magnesiodumortierite, a new mineral from very-high-pressure rocks (western Alps). II. Crystal chemistry and petrological significance. *European Journal of Mineralogy*, **7**, 525–535.

Foit, F.F., Jr., Fuchs, Y. and Myers, P.E. (1989) Chemistry of alkali-deficient schorls from two tourmaline-dumortierite deposits. *American Mineralogist*, **74**, 1317–1324.

Henry, D.J. and Dutrow, B.L. (1996) Metamorphic tourmaline and its petrologic applications. Pp. 500–555 in: *Boron Mineralogy, Petrology and Geochemistry* (E.S. Grew and L.M. Anovitz, editors). Reviews in Mineralogy, **33**. Mineralogical Society of America, Washington, D.C.

Hong, S.H. and Choi, P.Y. (1988) *Geological report of the Yuchon sheet (1:50,000)*. Korea Institute of Energy and Resources, Seoul, Korea, 26 pp.

Huijsmans, J.P.P., Barton, M. and van Bergen, M.J. (1982) A pegmatite containing Fe-rich grandidierite, Ti-rich dumortierite and tourmaline from the Precambrian, high-grade metamorphic complex of Rogaland, S.W. Norway. *Neues Jahrbuch für Mineralogie Abhandlungen*, **143**, 249–261.

Jin, M.S., Kim, S.J. and Shin, S.C. (1991) *Fission track and K-Ar ages of granites in southeastern Korea*. Report KR-90-1B2, Korea Institute of Energy and Resources. Taejon, Korea, pp. 57–98.

Kentgens, A.P.M. (1997) A practical guide to solid-state NMR of half-integer quadrupolar nuclei with some applications to disordered systems. *Geoderma*, **80**, 271–306.

Kerr, P.F. and Jenney, P. (1935) The dumortierite-andalusite mineralisation at Oreana, Nevada. *Economic Geology*, **30**, 287–300.

Kim, S.J., Kim, J.J. and Choo, C.O. (1992) Mineralogy and genesis of hydrothermal deposits in the southeastern part of Korean peninsula: (3) Miryang Napseok deposit. *Journal of Mineralogical Society of Korea*, **5**, 93–101.

Kim, Y. and Kirkpatrick, R.J. (1998) High-temperature multi-nuclear NMR investigation of analcime. *American Mineralogist*, **83**, 339–347.

Kirkpatrick, R.J. (1988) MAS-NMR spectroscopy of minerals and glasses. Pp. 341–403 in: *Spectroscopic Methods in Mineralogy and Geology* (F.C. Hawthorne, editor). Reviews in Mineralogy, **18**, Mineralogical Society of America, Washington, D.C.

Koh, S.M. and Chang, H.W. (1997) Comparative anatomy of the hydrothermal alteration of Chonnam and Kyongsang hydrothermal clay alteration areas in Korea. *Economic and Environmental Geology*, **30**, 81–87.

Koh, S.M., Tagaki, T., Kim, M.Y., Naito, K., Hong, S.S. and Sudo, S. (2000) Geological and geochemical characteristics of the hydrothermal clay alteration in south Korea. *Resources Geology*, **50**, 229–242.

Lee, K., Moo, H.-S., Song, Y. and Kim, I.J. (1993) Wall rock alteration and genetic environment of the Milyrang pyrophyllite deposit. *Journal of Korea Institute of Mining Geology*, **26**, 289–309.

Lippmaa, E., Samson, A. and Mägi, M. (1986) High-resolution ^{27}Al NMR of aluminosilicates. *Journal of the American Chemical Society*, **108**, 1730–1735.

Min, K.D., Kim, O.J., Lee, D.S. and Choo, S.H. (1982) Applicability of plate tectonics to the post Late Cretaceous igneous activities and mineralization in southern part of South Korea (I). *Journal of the Korea Institute of Mining Geology*, **15**, 123–154.

Moore, P.B. and Araki, T. (1978) Dumortierite, $Si_3B[Al_{6.75}O_{0.25}O_{17.25}(OH)_{0.75}]$: a detailed structure analysis. *Neues Jahrbuch für Mineralogie Abhandlungen*, **132**, 231–241.

Oh, D.G. and Chon, H.T. (1993) Geochemical dispersion of elements in volcanic wallrocks of pyrophyllite deposits in Milyang area, Kyeongnam province. *Journal of Korea Institute of Mining Geology*, **26**, 337–347.

Platonov, A.N., Langer, K., Chopin, C., Andrut, M. and Taran, M.N. (2000) Fe^{2+}–Ti^{4+} charge-transfer in dumortierite. *European Journal of Mineralogy*, **12**, 521–528.

Putnis, A., Fyfe, C.A. and Gobbi, G.C. (1985) Al, Si ordering in cordierite using magic angle spinning NMR. I: Si-29 spectra of synthetic cordierites. *Physics and Chemistry of Minerals*, **12**, 211–216.

Sabzehei, M. (1971) Dumortierite from Iran: a first record. *Mineralogical Magazine*, **38**, 526–527.

Schreyer, W., Abraham, K. and Behr, H.J. (1975) Sapphirine and associated minerals from kornerupine rock of Waldheim, Saxony. *Neues Jahrbuch für Mineralogie Abhandlungen*, **126**, 1–27.

Schreyer, W., Wodara, U., Marler, B., van Aken, P.A., Seifert, F. and Robert, J.-L. (2000) Synthetic tourmaline (olenite) with excess boron replacing silicon in the tetrahedral site: I. Synthesis conditions, chemical and spectroscopic evidence. *European Journal of Mineralogy*, **12**, 529–541.

Slack, J.F. (1996) Tourmaline associations with hydrothermal ore deposits. Pp. 559–643 in: *Boron Mineralogy, Petrology and Geochemistry* (E.S. Grew and L.M. Anovitz, editors). Reviews in Mineralogy, **33**. Mineralogical Society of America, Washington, D.C.

Tagg, S.L., Cho, H., Dyar, M.D. and Grew, E.S. (1999) Tetrahedral boron in naturally occurring tourmaline. *American Mineralogist*, **84**, 1451–1455.

Takahata, H. and Uchiyama, K. (1985) Dumortierite-bearing argillaceous gneisses from the Abukuma metamorphic terrain, northeast Japan. *Journal of Faculty of Science, Hokkaido University, Service IV*, **21**, 465–481.

Taner, M.F. and Martin, R.F. (1993) Significance of dumortierite in an aluminosilicate-rich alteration zone, Louvicourt, Quebec. *The Canadian Mineralogist*, **31**, 137–146.

Turner, G.L., Smith, K.A., Kirkpatrick, R.J. and Oldfield, E. (1985) Boron-11 nuclear magnetic resonance spectroscopic study of borate and borosilicate minerals and a borosilicate glass. *Journal of Magnetic Resonance*, **67**, 544–550.

Visser, D. and Senior, A. (1991) Mg-rich dumortierite in cordierite-orthoamphibole-bearing rocks from the high-grade Bamble Sector, south Norway. *Mineralogical Magazine*, **55**, 563–577.

Werding, G. and Schreyer, W. (1990) Synthetic dumortierite: its PTX-dependent compositional variations in the system Al_2O_3-B_2O_3-SiO_2-H_2O. *Contributions to Mineralogy and Petrology*, **105**, 11–24.

Werding, G. and Schreyer, W. (1996) Experimental studies on borosilicates and selected borates. Pp. 117–163 in: *Boron Mineralogy, Petrology and Geochemistry* (E.S. Grew and L.M. Anovitz, editors). Reviews in Mineralogy, **33**. Mineralogical Society of America, Washington, D.C.

Xue, X. and Kanzaki, M. (1998) Correlations between ^{29}Si, ^{17}O and ^{1}H NMR properties and local structures in silicates: an ab initio calculation. *Physics and Chemistry of Minerals*, **26**, 14–30.

[*Manuscript received 17 January 2003: revised 28 April 2003*]